Diffusion Coefficients in Hydrocarbon Systems

n-Heptane in the Gas Phase of the Methane–*n*-Heptane System

H. H. REAMER and B. H. SAGE
Chemical Engineering Laboratory, California Institute of Technology Pasadena, Calif.

Measurements of the molecular transport of *n*-heptane in the gas phase of the methane–*n*-heptane system under steady-state conditions have been made. Data were obtained at pressures up to approximately 2000 p.s.i.a. in the temperature interval between 100° and 220° F. The equipment employed is described and the results are presented in graphical and tabular form.

MOLECULAR TRANSPORT of materials in the gas phase has been the subject of much investigation. Fick's early work (*8*) coupled with more recent studies utilizing high pressure techniques by Drickamer (*15, 18, 19*) illustrate the steady-state and transient methods employed in this field. More recently, Schlinger (*17*) used the steady-state method for studying the molecular transport of several hydrocarbons in the gas phase of binary systems at pressures up to 100 p.s.i.a. Schlinger's methods have been adapted to high pressure measurements for this work. As an example of the type of experimental work available, recent work by others is mentioned on molecular transport of hydrocarbons and carbon dioxide in the gas phase.

Carmichael investigated the transport of *n*-heptane in the gas phase of the methane–*n*-heptane (*5*) and in the ethane–*n*-heptane and propane–*n*-heptane systems (*6*). Schlinger studied the transport of *n*-heptane in the air–*n*-heptane system (*17*). These studies were made at temperatures between 100° and 200° F. and for pressures up to 100 p.s.i.a., measurements were carried out under steady conditions. Berry (*3*) reported measurements on diffusion in mixtures of hydrogen-nitrogen, methane-ethane, nitrogen-ethane, and nitrogen-methane.

Drickamer (*15*) studied the self-diffusion of carbon dioxide at pressures up to 2250 p.s.i.a. while Amdur and co-workers (*1*) studied the diffusion of carbon dioxide in the carbon dioxide–nitrous oxide system near atmospheric pressure. Walker (*20*) studied the diffusion coefficient for carbon dioxide in the ternary carbon dioxide–helium–nitrogen system. O'Hern and Martin (*9*) reported values for the self-diffusion of carbon dioxide at pressures up to 3000 p.s.i.a. It is beyond the scope of this work to review further experimental work in gaseous diffusion.

METHODS AND APPARATUS

In principle, the method follows Schlinger's (*17*). The earlier measurements by Schlinger were carried out in an effort to determine the feasibility of such an approach to molecular transport measurements in the gas phase at elevated pressures. The transport path takes place in that portion of the cylindrical vessel shown in the right side of Figure 1 at *A*. The lower part of the vessel contains a porous plate of sintered glass shown at *B*. This porous plate has a capillary pressure of approximately 5 p.s.i. with conventional hydrocarbons at atmospheric pressure. The less volatile component of the binary system is evaporated from the porous plate. To establish the existence of steady state, an aneroid-type diaphragm with a sensitivity of the order of 0.2 p.s.i. is installed below the porous plate at *C*. A linear transducer of the reluctance type is placed below

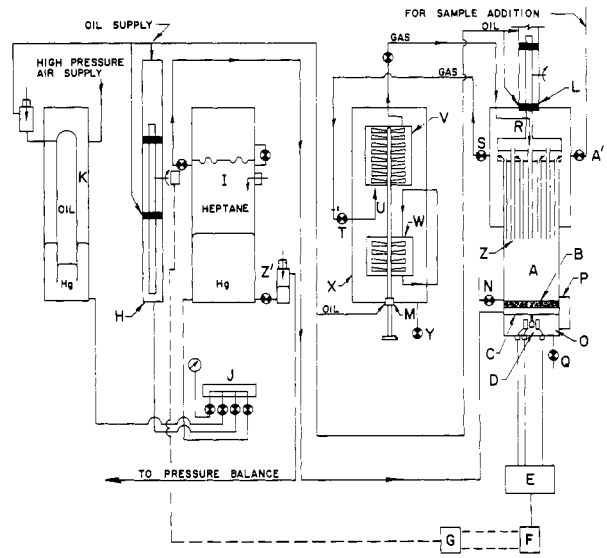

Figure 1. Schematic diagram of apparatus

the diaphragm at *D* and is connected to external equipment as has been described for high-pressure manostats (*13, 14*). After appropriate amplification at *E* by balanced diodes, the vector output is fed into the galvanometer *F* which, in turn, operates through an optical lever the modulator *G* that controls the operation of the injector *H*. Since the aneroid diaphragm *C* is fully pressure-compensated, changes in the capillary pressure on the upper surface of the porous plate *B* are reflected in the output of the transducer *D* which is transmitted through the appropriate electronic and optical linkages to the modulator *G* and thus control the speed of injection of the liquid hydrocarbon in *H*.

The hydrocarbon is confined over mercury in the lower part of the chamber *I*. This chamber is maintained at a constant temperature of 130° F. The mercury is introduced from the injector *H* through the valve assembly *J* which is so arranged that large changes in the quantity of mercury in the system may be accomplished by transfers to or from the vessel *K*. This vessel also supplies oil to the pressure-compensated packing and plunger of the injector *H* (*11*). The arrangement of the vessel *I* and the injector *H* with the associated pressure vessel *K* has been described (*13, 14*). Likewise, this compensating oil pressure is provided to the packing gland *L* in the upper part of the vessel *A* and into the cylinder-sleeve combination *M* (*11*). The assembly thus permits the less volatile component, which is liquid at the temperature and pressure existing at *A*, to be introduced at

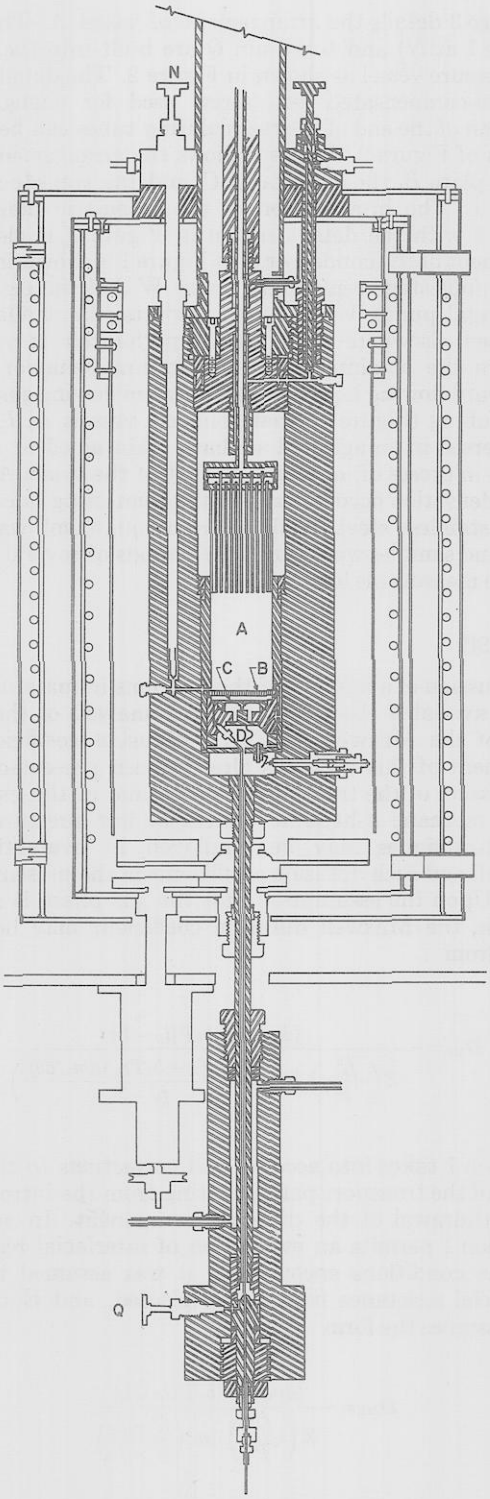

Figure 2. Details of transport vessel

a steady rate just equal to the rate of evaporation at B. The diffusion of the stagnant component into the liquid interstices of the porous plate takes place during the initiation of the transport process until such a rate is established to yield a steady situation. Under these conditions, the rate of diffusion of the more volatile component is just equal to the rate of transport to the surfaces of the plate by the gross motion of the fluids existing therein.

To avoid the gradual accumulation of impurities at the surface of the porous plate B, provision is made for flooding the lower part of the chamber A and withdrawing

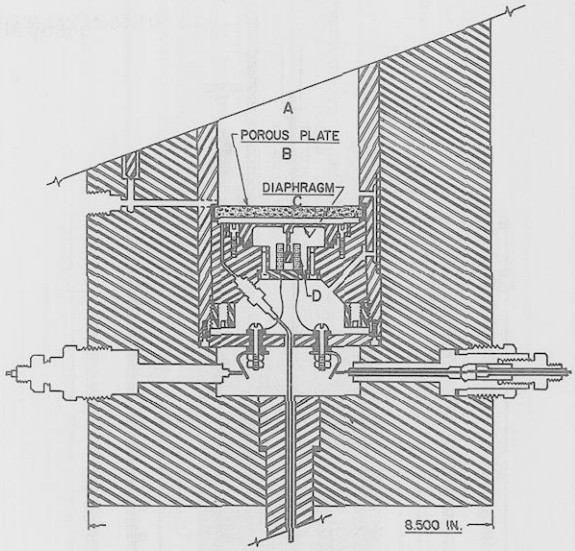

Figure 3. Details of porous plate

the liquid phase through the valve N. This arrangement has proven satisfactory for a variety of less volatile components. Special pressure compensation from the gas phase of the vessel A to the gas phase in the area O is provided by the small line P. A drain is provided at Q to permit cleaning the equipment without disassembly. The upper part of the transport path in A is filled with a bundle of some 500 small tubes approximately 0.050 inch in diameter. These tubes are closely packed and so arranged that gas is introduced at R, passed downward through the tubes, upward through the annular space around each tube, and out of the vessel A through the valve S. The gas returns to the absorber through valve T where it passes upward through streams of liquid at U, is compressed by the eight-stage centrifugal pump V, and returned to the vessel A at R. Circulation of liquid through the absorber U is accomplished by the four-stage centrifugal pump W. Provision is made for the gradual withdrawal of the increase in volume of liquid in the chamber X at Y. The latter vessel is maintained at a somewhat lower temperature than the vessel A. This provides for the return of gas at R of a fixed composition differing somewhat from the equlibrium composition at the surface of the plate B in the vessel A. Provisions are made at U to permit close contact between the upward flowing gas and the downward flowing dispersed liquid. Experimental measurements established that the gas returning at R is in substantial equilibrium with the recirculating liquid in X. Therefore, from a knowledge of the temperature and pressure existing at U and information as to the available phase equilibrium involved, the composition of the fluid entering the upper part of A is known. From the available volumetric data and the composition of the phase, direct evaluation of the concentration component can be made.

The composition of the gas leaving the vessel A at S is slightly richer in the less volatile component as a result of the transport process in A. An appropriate small correction to obtain the effective concentration of each of the components of the binary system was made at Z. The equipment is so arranged that the length of the transport path can be changed from 0.75 to 4.5 inches by raising or lowering the bundle of tubes shown in the upper part of A and terminating at Z. The temperature of the porous plate is known by means of thermocouples imbedded in the sintered glass plate. An electrical heater beneath the porous plate supplies electrical energy when necessary to maintain the surface of the plate B at the same temperature as the remainder of vessel A.

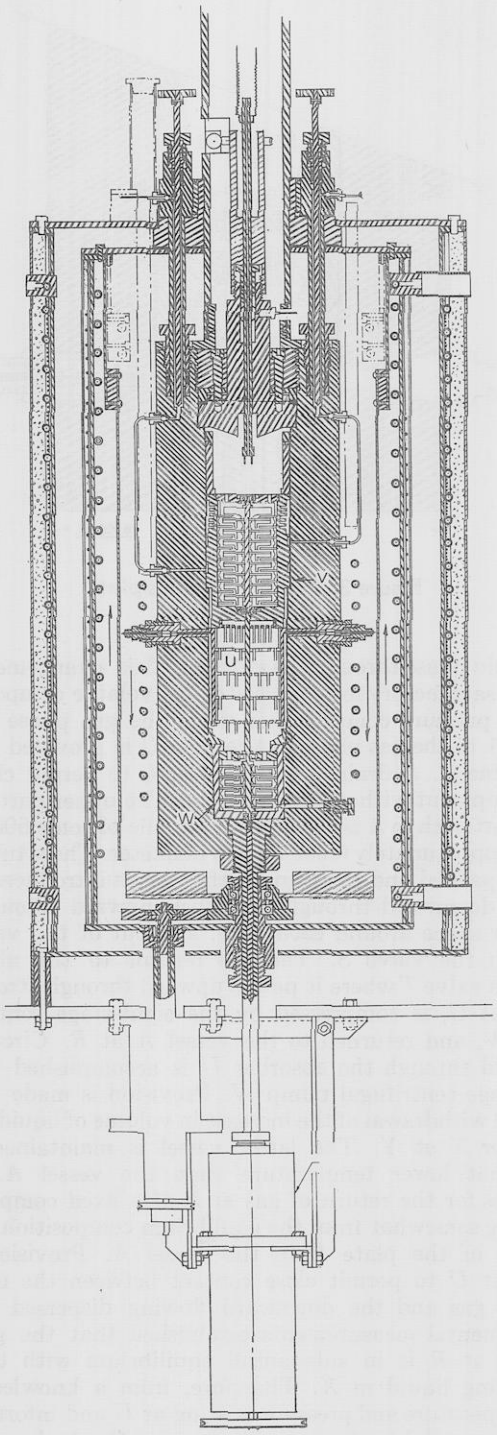

Figure 4. Details of condenser

Concentrations of the diffusing and stagnant components are known at B from the pressure and temperature existing in the vessel A. Similarly, a concentration of each of the components is known at Z from the pressure and temperature existing in the vessel X. Each vessel is immersed in an agitated oil bath.

The temperature of the vessels A, I, and X was known within 0.02° F. of the international platinum scale, and fluctuations of steady state greater than 0.005° F. are uncommon. Pressure in the vessel A is determined through the mercury-oil interface at Z' by means of a pressure balance (*4, 16*) which was calibrated against the vapor pressure of carbon dioxide at the ice point. Corrections for the diviations from zero capillary pressure on the surface of B are made in arriving at the equilibrium pressure at A.

Figure 2 details the arrangement of vessel A. The valve (Figure 1 at N) and the drain Q are built into the wall of this pressure vessel as shown in Figure 2. The details of the pressure-compensated lead screw used for changing the elevation of the end of the recirculating tubes can be seen in the top of Figure 2. Figure 3 shows the arrangement of the porous plate B, the diaphragm C, and the transducer D of Figure 1. The interrelation of the schematic diagram of Figure 1 with the details shown in Figure 3 is clear. Arrangement of the condenser U of Figure 1 is shown in Figure 4. The four-stage centrifugal pump W and the eight-stage centrifugal pump V are in all respects like similar units described elsewhere (*12*). Small perforated trays at U improve the attainment of equilibrium behavior in the downward flowing liquid and the upward flowing gas.

All tubing (Figure 1) that connects vessels A, I, and X is immersed in an agitated air bath maintained at a temperature in excess of, or equal to, that of the vessel A. Thus, no condensation occurs in any of the connecting lines, which are of stainless steel. Leakage from equipment was negligible, and samples were stored for periods of several months with no measurable loss.

ANALYSIS

Discussion of a number of the relations in material transport is available elsewhere (*10*). An analysis of the evaluation of the Maxwell and Fick diffusion coefficients for equipment of this type has already been presented (*7*) in a discussion of the transport of n-heptane in the gas phase of the methane–n-heptane system at low pressures. The same techniques may be employed in evaluating the Maxwell and Fick diffusion coefficients in the present equipment. Upon the assumption that the gas phase is an ideal solution, the Maxwell diffusion coefficient may be established from

$$D_{Mk} = -\frac{(dm_k/d\theta)\, b_k T (l_G - l_c)}{Z\left(\frac{f_k^0}{P}\right) \ln\left(\frac{f_k^0 - f_{ki} + b_k T r_{ki}(dm_k/d\theta)}{f_k^0 - f_{kt}}\right)} \qquad (1)$$

Equation 1 takes into account end corrections to the gross length of the transport path resulting from the introduction and withdrawal of the diffusing component. In addition, Equation 1 permits an evaluation of interfacial resistance. For the conditions encountered it was assumed that the interfacial resistance could be neglected, and Equation 1 then assumes the form

$$D_{Mk} = -\frac{(dm_k/d\theta)\, b_k T (l_G - l_c)}{Z\left(\frac{f_k^0}{P}\right) \ln\left(\frac{f_k^0 - f_{ki}}{f_k^0 - f_{kt}}\right)} \qquad (2)$$

The magnitude of the end corrections was established from measurements made at the same state with two different transport lengths. This will permit the elimination of the length correction and the direct evaluation of the Maxwell diffusion coefficient.

If the gas phase is assumed to be a perfect gas, a simpler expression (Equation 3) is obtained which is more readily evaluated from available information, and may be just as useful.

$$D_{Mk} = -\frac{(dm_k/d\theta)\, b_k T (l_G - l_c)}{\ln(n_{ji}/n_{jt})} \qquad (3)$$

The Fick diffusion coefficient may be readily established from the following integrated form involving only the diffusional transport rate $dm_{kd}/d\theta$:

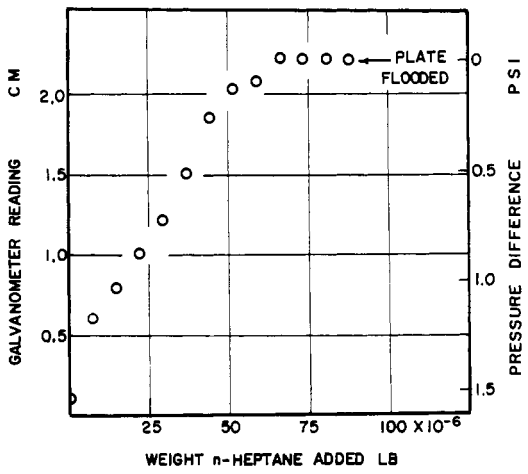

Figure 5. Capillary pressure of porous plate

$$D_{Fk} = \frac{(dm_{kd}/d\theta)}{(\partial\sigma_k/\partial l)} = \frac{(dm_{kd}/d\theta)(l_G - l_c)}{(\sigma_{ki} - \sigma_{kt})}$$

$$= \frac{[(dm_k/d\theta) - u\sigma_k][l_G - l_c]}{(\sigma_{ki} - \sigma_{kt})} \qquad (4)$$

In carrying out the integration shown in the second equality the Fick diffusion coefficient was assumed to be a constant over the range of conditions involved in the transport path. Equation 4 includes a term for the hydrodynamic velocity. This may be eliminated by appropriate rearrangement of Equation 4 and by making use of the basic relationships of material transport.

$$D_{Fk} = \frac{(dm_k/d\theta)\sigma_j}{\sigma_k(\partial\sigma_k/\partial l)} \approx \frac{\sigma_j^*(dm_k/d\theta)(l_G - l_c)}{\sigma^*(\sigma_{ki} - \sigma_{kt})} \qquad (5)$$

Equation 5 is the expression employed in the evaluation of the Fick diffusion coefficient from the experimental measurements. The values of the concentration are obtained from available volumetric data (*5*), while the material flux of the *n*-heptane is established from the experimental measurements. The deviations from an ideal solution of the gas phase in the methane–*n*-heptane system are sufficient to make the utility of Equations 1 to 3 questionable; no Maxwell coefficients have been reported.

MATERIALS

Research-grade *n*-heptane was obtained from the Phillips Petroleum Co. and was reported to contain less than 0.0011 mole fraction of material other than *n*-heptane. This hydrocarbon exhibited a specific weight at 77° F. on an air-free basis of 42.4153 pounds per cubic foot which compares with a value of 42.419 pounds per cubic foot reported by Rossini (*2*) for an air-saturated sample. The index of refraction relative to the D-lines of sodium at 77° F. was 1.38511 as compared to a value of 1.38511 reported by Rossini for the same temperature and for an air-saturated sample. From the agreement of these values it is believed that the *n*-heptane contained less than 0.001 mole fraction of impurities. The purity of the *n*-heptane was confirmed by the steady rates of evaporation from the porous plate *B* in Figure 1 for extended periods. The *n*-heptane identified as pure grade used in the condenser was obtained from the Phillips Petroleum Co. and exhibited a specific weight of 42.4286 pounds per cubic foot and an index of refraction of 1.3851.

The methane used in this investigation was obtained from a well in the San Joaquin Valley and was reported to contain less than 0.001 mole fraction of impurities. This hydrocarbon was passed over calcium chloride, Ascarite, anhydrous calcium sulphate, and freely activated charcoal at pressures in excess of 500 p.s.i.a.

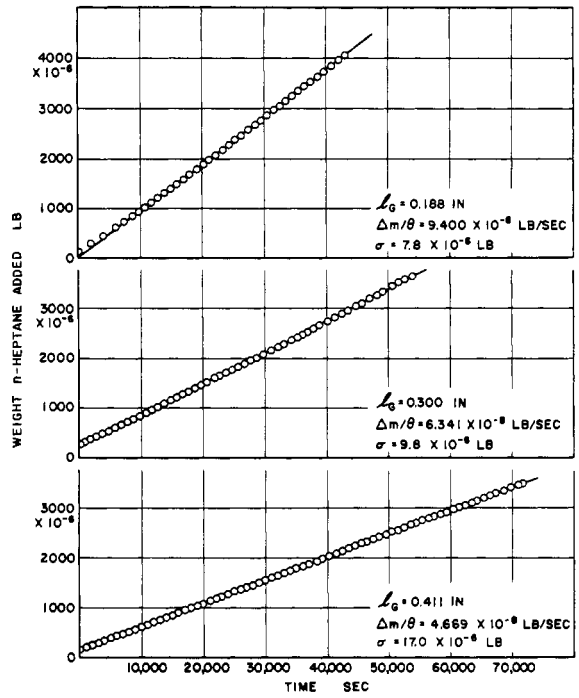

Figure 6. Illustrative experimental results

PROCEDURE

The *n*-heptane was introduced into the condenser *U* and into the vessel *A* by the conventional high-vacuum techniques also employed in filling the vessel *I* with *n*-heptane. Methane was introduced through valve *A'* in Figure 1 until the desired pressure was reached for the temperature of measurement. Circulation of the gas through the circuit involving the valve *S* by the centrifugal pump *V* was continued for a reasonable period to bring equilibrium. During this period, the injector *H* was so adjusted as to maintain a predetermined small capillary pressure on the surface of the plate *B*. As an indication of the sensitivity of the equipment, there is shown in Figure 5 the capillary pressure measured by the aneroid diaphragm *C* of Figure 3 as a function of the weight of *n*-heptane introduced from the injector *H* under equilibrium conditions when there was no transport from the vessel *A*. In Figure 5 the capillary pressure is expressed in terms of the reading of the galvnometer which is associated with the transducer *D* of Figure 3 as well as in conventional units.

The equipment was then placed on automatic control with the constant speed drive of the centrifugal pumps in the vessel *X* controlled within approximately 5° or 0.05%, whichever was the larger measure of uncertainty, by a speed control system (*13*). The feedback control from the diaphragm *C* to the injector *H* functions satisfactorily. A print readout attached to the worm drive of the injector *H* records the amount of *n*-heptane injected as a function of time. The control point is usually maintained as indicated in Figure 5. This may be readily adjusted by appropriate compensation in the electronic circuits of *E* of Figure 1.

A sample set of three different experimental results obtained at 978 p.s.i.a. and 160° F. is shown in Figure 6. The standard error of estimate of the points shown from a straight line for each of the three sets of data is indicated on the diagram. In calculating the standard error of estimate it was assumed that there was no error in time and all

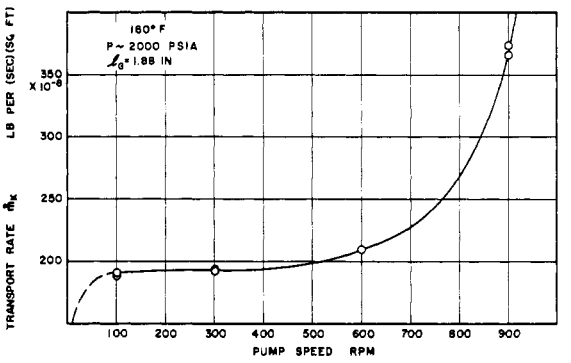

Figure 7. Effect of gas circulation rate upon transport

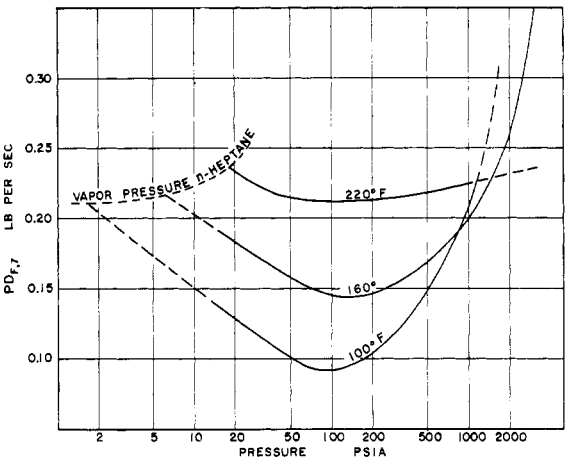

Figure 8. Fick diffusion coefficient for n-heptane in a mixture containing 0.9 weight fraction methane

the uncertainty was in the weight of n-heptane introduced from the injector H. The slope of this line obtained in the course of least squares evaluation is also presented in Figure 6.

From measured rates of transport at the three different path lengths for the same state it is possible to take into account the end correction resulting from gross motion at the interface B in the vessel A of Figure 1 and other end effects not fully evaluated otherwise. The use of three sets of data permits a check on this situation. Agreement within 0.5% between data obtained at three different lengths was possible.

Figure 7 presents the influence of the speed of rotation of the pumps in vessel X upon the transport rate in A. The transport rate is relatively insensitive to the speed of rotation until a value of 400 r.p.m. has been reached. At that point, apparently a critical Reynolds number is reached at the interface B, and marked influence of the speed of rotation, and hence of the velocity of the gas emerging from the tube bundle at the upper part of the vessel A, is realized. Therefore, it is desirable to keep all measurements at speeds below this critical Reynolds number. Throughout this work, all measurements were made at speeds of rotation of the pumps in the vessel X at less than half the critical value of the Reynolds number which was illustrated in Figure 7. Furthermore, measurements were made of at least two pump speeds for nearly all states in order to determine independently that the effect of the pump speed was not marked.

The proper speed of rotation was approximated from the following expression which was based on the assumption that the Reynolds number of the flow at the exit of the pump controls the length correction:

$$s = (\mathrm{Re}k)^{1/2} \frac{ZT_n}{P} \tag{6}$$

Information concerning the specific weight of the fluid was available. Equation 6 assumes that the rate of flow is directly proportional to the square of the velocity, and that the viscosity was invariant from that predicted at atmospheric pressure.

EXPERIMENTAL RESULTS

Table I reports all experimental results obtained on the study of the transport of n-heptane in the gas phase of the methane–n-heptane system. The data submitted include prevailing pressure and temperature in the vessels A and X, the length of the transport path, and the weight rate of injection of n-heptane, together with the standard deviation. In most cases something over 200 values of the quantity of n-heptane as a function of time were established for each set of measurements. The slope and standard error of estimate were evaluated from data shown in Figure 6 by standard least squares techniques on automatic computing equipment. Table I sets forth for each of the experimental points, values of the concentration for n-heptane at B and Z of Figure 1 and the corresponding gross and net length of the transport path.

Figure 8 presents the effect of pressure upon the Fick diffusion coefficient of n-heptane for the several temperatures investigated for a weight fraction methane of 0.9. Smoothed values for the transport of n-heptane in the gas phase of the methane–n-heptane system are set forth in Table II for the different weight fractions methane. The standard deviation of the experimental data and the precision with which each of the numerous variables was evaluated lead the authors to believe that these transport data, which are in excellent agreement with the earlier measurements of Schlinger (*17*), do not involve uncertainties greater than 2%. It is always disappointing in measurements involving a large number of variables to find the need for the maintenance of steady state with a precision of 0.1% and an accuracy of not more than 0.2% in each of the variables in order to obtain a result with an over-all uncertainty of the order of 2%.

ACKNOWLEDGMENT

This work is a contribution from the American Petroleum Institute Research Project 37 at the California Institute of Technology. Equipment was developed over a period of years with the assistance of W.M. DeWitt, George Griffith, and L.S. Wood in connection with the construction and drafting activities. John Lower contributed to the experimental measurements, Virginia Berry assisted with calculations, and Carol Lovelady with preparation of the manuscript.

NOMENCLATURE

b	=	specific gas constant, ft./° R.
D_{Fk}	=	Fick diffusion coefficient of component k, sq. ft./sec.
D_{Mk}	=	Maxwell diffusion coefficient of component k, lb./sec.
d	=	differential operator
f	=	fugacity, lb./sq. ft.
k	=	constant of proportionality
l	=	effective transport length, ft.
l_c	=	effective correction to gross transport length, ft.
l_G	=	gross transport length, ft.
ln	=	natural logarithm
$dm_k/d\theta$	=	transport rate of component k, lb./(sec.)(sq. ft.)
m_k	=	weight of component k, lb.
N	=	number of experimental points

Table I. Experimental Results for *n*-Heptane in Gas Phase of the Methane–*n*-Heptane System

Pressure, P.S.I.A.	Transport Rate,[a] Lb./(sec.)(sq. ft.)	Standard Error of Estimate,[b] Lb.	Concentration *n*-Heptane, Lb./cu. ft. Interface	Concentration *n*-Heptane, Lb./cu. ft. Terminal	Length, Ft. Gross	Length, Ft. Net	Fick Diffusion Coefficient, Sq. ft./sec.	Deviation[c] Fraction
				100° F.				
983	54.60×10^{-8}	11.1×10^{-6}	0.162	0.112	0.1882	0.1514	0.0158×10^{-4}	−0.026
972	51.54	5.0	0.161	0.110	0.1882	0.1517	0.0150	0.026
				160° F.				
980	191.50×10^{-8}	7.8×10^{-6}	0.312	0.111	0.1882	0.1514	0.0134×10^{-4}	0.043
982	184.79	12.0	0.312	0.112	0.1882	0.1610	0.0138	0.014
982	181.80	3.1	0.312	0.112	0.1882	0.1708	0.0144	−0.029
980	185.32	6.7	0.312	0.111	0.1882	0.1707	0.0146	−0.043
980	200.84	5.0	0.312	0.111	0.1882	0.1514	0.0140	0
1925	196.06×10^{-8}	9.5×10^{-6}	0.933	0.609	0.1882	0.1713	0.00914×10^{-4}	−0.002
1929	196.01	6.6	0.937	0.614	0.1882	0.1713	0.00916	−0.004
1850	85.51	2.9	0.857	0.529	0.4114	0.3955	0.00916	−0.004
1788	83.72	4.0	0.800	0.472	0.4114	0.3956	0.00901	0.012
2770	202.99×10^{-8}	6.6×10^{-6}	2.580	2.225	0.1882	0.1645	0.00734×10^{-4}	−0.022
2750	182.87	6.0	2.535	2.200	0.1882	0.1645	0.00703	0.021
				220° F.				
1076	631.72×10^{-8}	246.2×10^{-6}	0.690	0.129	0.1882	0.1488	0.0146×10^{-4}	0.007
1075	662.27	186.3	0.689	0.129	0.1882	0.1488	0.0153	−0.041
1087	250.81	18.4	0.698	0.130	0.4114	0.3719	0.0143	0.027
1080	250.75	13.7	0.692	0.130	0.4114	0.3720	0.0145	0.014

[a] Effective cross sectional area = 0.04909 sq. ft. [b] Standard error of estimate, $\sigma = [\{\sum(\Delta m_e - \Delta m_s)^2\}/(N-1)]^{1/2}$. [c] Fractional deviation = $[(D_{Fn})_a - (D_{Fn})_e]/(D_{Fn})_a$.

Table II. Diffusion Coefficients for *n*-Heptane for Average Conditions

Pressure, P.S.I.A.	Compn. Wt. Fraction Methane	Diffusion Coeff. *n*-Heptane, Sq. Ft./Sec.	Pressure, P.S.I.A.	Compn. Wt. Fraction Methane	Diffusion Coeff. *n*-Heptane, Sq. Ft./Sec.
		100° F.[a]			
14.696	0.8	0.581×10^{-4}	500	0.8	0.0160×10^{-4}
	0.9	0.647		0.9	0.0205
	1.0	0.704		1.0	0.0203
20	0.8	0.396×10^{-4}	1000	0.8	0.0126×10^{-4}
	0.9	0.441		0.9	0.0143
	1.0	0.486		1.0	0.0158
40	0.8	0.163×10^{-4}	1500	0.8	0.0110×10^{-4}
	0.9	0.186		0.9	0.0128
	1.0	0.203		1.0	...
60	0.8	0.0984×10^{-4}	2000	0.8	0.00975×10^{-4}
	0.9	0.111		0.9	...
	1.0	0.119		1.0	...
100	0.8	0.0549×10^{-4}	2500	0.8	0.00863×10^{-4}
	0.9	0.0639		0.9	...
	1.0	0.0660		1.0	...
200	0.8	0.0278×10^{-4}	3000	0.8	0.00780×10^{-4}
	0.9	0.0361		0.9	...
	1.0	0.0351		1.0	...
		160° F.			
14.696	0.8	0.813×10^{-4}	500	0.8	0.0197×10^{-4}
	0.9	0.898		0.9	0.0233
	1.0	0.978		1.0	0.0254
20	0.8	0.566×10^{-4}	1000	0.8	0.0119×10^{-4}
	0.9	0.632		0.9	0.0138
	1.0	0.688		1.0	0.0151
40	0.8	0.252×10^{-4}	1500	0.8	0.00773×10^{-4}
	0.9	0.283		0.9	0.0106
	1.0	0.314		1.0	0.0116
60	0.8	0.151×10^{-4}	2000	0.8	0.00736×10^{-4}
	0.9	0.176		0.9	0.00903
	1.0	0.199		1.0	0.00990
100	0.8	0.0875×10^{-4}	2500	0.8	0.00638×10^{-4}
	0.9	0.1000 ×		0.9	0.00836
	1.0	0.113		1.0	0.00908
200	0.8	0.0430×10^{-4}	3000	0.8	0.00574×10^{-4}
	0.9	0.0507		0.9	0.00799
	1.0	0.0559		1.0	0.00884
		220° F.[a]			
20	0.8	0.729×10^{-4}	1000	0.8	0.0125×10^{-4}
	0.9	0.807		0.9	0.0155
	1.0	0.878		1.0	0.0169
40	0.8	0.337×10^{-4}	1500	0.8	0.00833×10^{-4}
	0.9	0.377		0.9	0.0105
	1.0	0.415		1.0	0.0119
60	0.8	0.219×10^{-4}	2000	0.8	0.00626×10^{-4}
	0.9	0.246		0.9	0.00802
	1.0	0.269		1.0	0.00929
100	0.8	0.128×10^{-4}	2500	0.8	0.00502×10^{-4}
	0.9	0.147		0.9	0.00647
	1.0	0.155		1.0	0.00767
200	0.8	0.0632×10^{-4}	3000	0.8	0.00418×10^{-4}
	0.9	0.0738		0.9	0.00544
	1.0	0.0750		1.0	0.00654
500	0.8	0.0251×10^{-4}			
	0.9	0.0302			
	1.0	0.0312			

[a] Values of the Fick diffusion coefficient for *n*-heptane at pressures greater than 1000 p.s.i.a. are extrapolated and have a larger uncertainty than those at the lower pressures.

n_j = mole fraction component j
n_j = weight fraction component j
P = pressure, lb./sq. ft. abs., or p.s.i.a.
Re = Reynolds number
r_i = interfacial resistance, sec./ft.
s = speed of rotation, r.p.m.
T = thermodynamic temperature, ° R.
u = hydrodynamic velocity, ft./sec.
Z = compressibility factor of gas phase
Δ = difference in
η = absolute viscosity, lb. sec./sq. ft.
θ = time, sec.
Σ = summation operator
σ = specific weight of phase, lb./cu. ft.
σ_k = concentration of component k, lb./cu. ft.
∂ = partial differential operator

Subscripts

av = average
d = diffusion
e = experimental
i = conditions at interface
j, 1 = stagnant component, methane
k, 7 = diffusing component, n-heptane
n = index
s = smooth
t = conditions at exit of transfer section (terminal)

Superscripts

0 = pure state
* = average

LITERATURE CITED

(1) Amdur, I., Irvine, J.W., Jr., Mason, E.A., Ross, J., *J. Chem. Phys.* **20**, 436 (1952).
(2) Am. Petrol. Proj. 44, Petrol. Res. Lab., Carnegie Inst. Technol., "Selected Values of Properties of Hydrocarbons and Related Compounds."
(3) Berry, V.J., Jr., Koeller, R.C., "Diffusion in Compressed Binary Gaseous Systems," A.I.Ch.E. Joint Symposium on Nonequilibrium Fluid Mechanics, Kansas City, 1959.
(4) Bridgeman, O.C., *J. Am. Chem. Soc.* **49**, 1174 (1927).
(5) Carmichael, L.T., Reamer, H.H., Sage, B.H., Lacey, W.N., *Ind. Eng. Chem.* **47**, 2205 (1955).
(6) Carmichael, L.T., Sage, B.H., *A.I.Ch.E.J.* **2**, 273 (1956).
(7) Carmichael, L.T., Sage, B.H., Lacey, W.N., *Ibid.*, **1**, 385 (1955).
(8) Fick, Adolf, *Ann. Phys.* **94**, 59 (1855).
(9) O'Hern, H.A., Jr., Martin, Joseph, J., *Ind. Eng. Chem.* **47**, 2081 (1955).
(10) Opfell, J.B., Sage, B.H., *Ibid.*, **47**, 918 (1955).
(11) Reamer, H.H., Opfell, J.B., Sage, B.H., *Ibid.*, **48**, 275 (1956).
(12) Reamer, H.H., Richter, G.N., DeWitt, W.M., Sage, B.H., *Trans. Am. Soc. Mech. Engrs.* **80**, 1004 (1958).
(13) Reamer, H.H., Sage, B.H., *Rev. Sci. Instr.* **24**, 362 (1953).
(14) *Ibid.*, **29**, 709 (1958).
(15) Robb, W.L., Drickamer, H.G., *J. Chem. Phys.* **19**, 1504 (1951).
(16) Sage, B.H., Lacey, W.N., *Trans. Am. Inst. Mining Met. Engrs.* **136**, 136 (1940).
(17) Schlinger, W.G., Reamer, H.H., Sage, B.H., Lacey, W.N., API Biennial Vol., 70-106 (1952-53).
(18) Scott, E.J., Tung, L.H., Drickamer, H.G., *J. Chem. Phys.*, **19**, 1075 (1951).
(19) Timmerhaus, K.D., Drickamer, H.G., *Ibid.*, **20**, 981 (1952).
(20) Walker, R.E., DeHaas, N., Westenberg, A.A., *Ibid.*, **32**, 1314 (1960).

RECEIVED for review April 30, 1962. Accepted September 17, 1962.

Heats of Formation of the Sparingly Soluble Iodates of Silver (I), Thallium (I), Lead (II), and Barium (II)

J. H. STERN, R. PARKER, L. S. PEAK, and W. V. VOLLAND
Department of Chemistry, Long Beach State College, Long Beach 4, Calif.

Heats of formation of sparingly soluble iodates were determined by combining measured heats of precipitation with auxiliary data necessary to correct the calorimetric results to standard states. The following values are reported for the standard heats of formation, ΔH^0_{f298} in kcal./mole: silver iodate (c), −41.6; thallium iodate (c), −65.7; lead iodate (c), −120.8 and barium iodate (c), −249.5.

THIS INVESTIGATION is part of a study in this laboratory (*5*, *6*) of thermodynamic properties of various oxidation states of iodine and its compounds. No heats of formation of these iodates are listed by the National Bureau of Standards (*3*). Latimer (*2*) gives only the heats of formation of $AgIO_3$ and $TlIO_3$.

Heats of precipitation in dilute aqueous solutions were measured for systems of the following type:

$$M^{x-}(aq) + xIO_3^-(aq) \rightarrow M(IO_3)_x \text{ (finely divided)};$$

where $M^{x-} = Ag^-, Tl^-, Pb^{2-}$, and Ba^{2-}.

These heats were combined with appropriate corrections to standard states and supporting thermodynamic data to yield heats of formation. The stoichiometry of the reactions is well established since the solubility of these iodates is very low (*2*, *4*).